Aspects of surface and interface characterizations by X-rays: The research programme at IOP, Bhubaneswar

B. N. Dev

Institute of Physics, Sachivalaya Marg, Bhubaneswar 751 005, India

Surface and interface studies constitute an important experimental research programme of the Institute of Physics, Bhubaneswar since 1991. In recent years, experimental techniques like high resolution X-ray diffraction (HRXRD), X-ray reflectometry (XRR) and X-ray standing wave (XSW) have been set up around an 18 kW rotating anode X-ray generator and Rutherford backscattering spectrometry and channelling have been set up around a 3 million volt tandem Van de Graaff ion accelerator (Pelletron). Besides the in-house facilities we also use facilities available elsewhere to study complementary aspects of specific research problems. The research programme mainly involves studies of surface modifications in ion–solid interaction, growth of epitaxial layers on surfaces, strain and defects in epilayers, interface atomic structure and adsorption/desorption on single crystal surfaces. In this article we present some examples of surface and interface characterizations with X-rays.

Surface modifications in ion–solid interaction

Surface and interface roughness

Ion–solid interaction causes various kinds of surface and near-surface modifications. Having set up the high resolution X-ray diffraction (HRXRD), X-ray reflectometry (XRR) and X-ray standing wave (XSW)[1,2] techniques, we studied the effect of ion irradiation on surface roughness. The XRR results in Figure 1 (from Satyam *et al.*[2]) show the enhancement of surface roughness (from 9.1 ± 1 to 14.5 ± 1 Å) upon 1.38 MeV Au^{2+} implantation into a $LiNbO_3$ (001) crystal.

Near-surface vacancy enrichment in ion–solid interaction

In a study of nonlinear effects in electronic excitation in energetic cluster–solid interaction, from post-irradiation XRR results (Figure 2) we observed the formation of a thin (< 10 nm) surface layer with lower electron density compared to the bulk value[3]. We attributed it to the formation of excess vacancies in this region due to heavy ion (Ga^{2+}) interaction with the solid (GaAs). TRIM[3,4] simulation also shows excess vacancies over this depth.

Growth of epilayers on vicinal surfaces

Vicinal surfaces of single crystals are often used to fabricate aligned epitaxial structures. We have used vicinal Si(111) surfaces (surface at an angle of 4° with respect to the (111) planes) for the growth of epitaxial layers and structures on them. The vicinal angle has been determined by the HRXRD technique[1]. Through self-assembled growth of epitaxial island structures on these surfaces we provided the first experimental results[5] on the predicted[6] phenomenon of *shape transition* in heteroepitaxial islands. Our quantitative analysis was later followed for other systems showing shape transition[7].

Epitaxial growth of overlayers on vicinal surfaces, because of the presence of atomic steps on the surface, usually introduces defects at the interface. This often tilts the orientation of the overlayer with respect to the substrate. There are theoretical results which are yet to be substantiated. We have grown epitaxial Ag(111) layers on vicinal (4° miscut) Si(111) surfaces. These are uniform thin (~ 100 nm) films. We used HRXRD measurements to determine the angle between Ag[111] and Si[111] crystallographic directions, average strain and the mosaic spread in the epilayers[8]. The sample configuration and the experimental geometry are shown in Figure 3 and the HRXRD results are shown in Figure 4. The measured angle ($\delta\psi = 0.31 \pm 0.01°$) between Ag[111] and Si[111] is in good agreement with that expected for a miscut angle of 4° (ref. 8).

Heteroepitaxial layers are strained because of different lattice parameters of the overlayer and the substrate materials. Shape transition, discussed earlier, is a mode of strain relaxation. There is another, more familiar, mode of strain relaxation in the epilayers, namely introduction of misfit dislocations. There is a critical thickness (t_c) of the epilayer up to which the layer grows

e-mail: bhupen@iopb.res.in

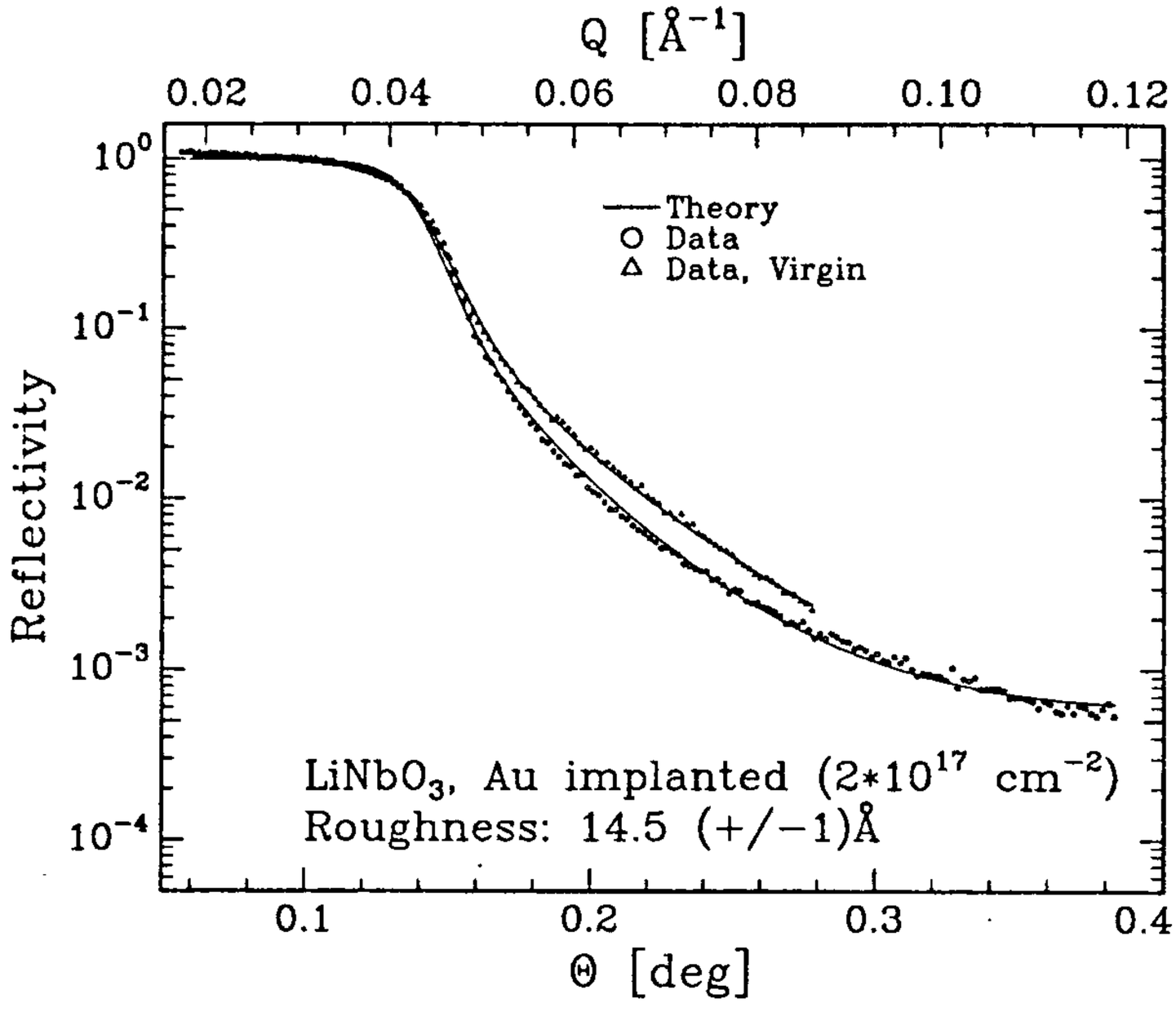

Figure 1. MoK$_{\alpha 1}$ X-ray (17.479 keV) reflectivity from an Au-implanted $LiNbO_3$(001) sample (O). For a comparison the reflectivity from a virgin sample (Δ) is also shown. (From Satyam *et al.*[2]).

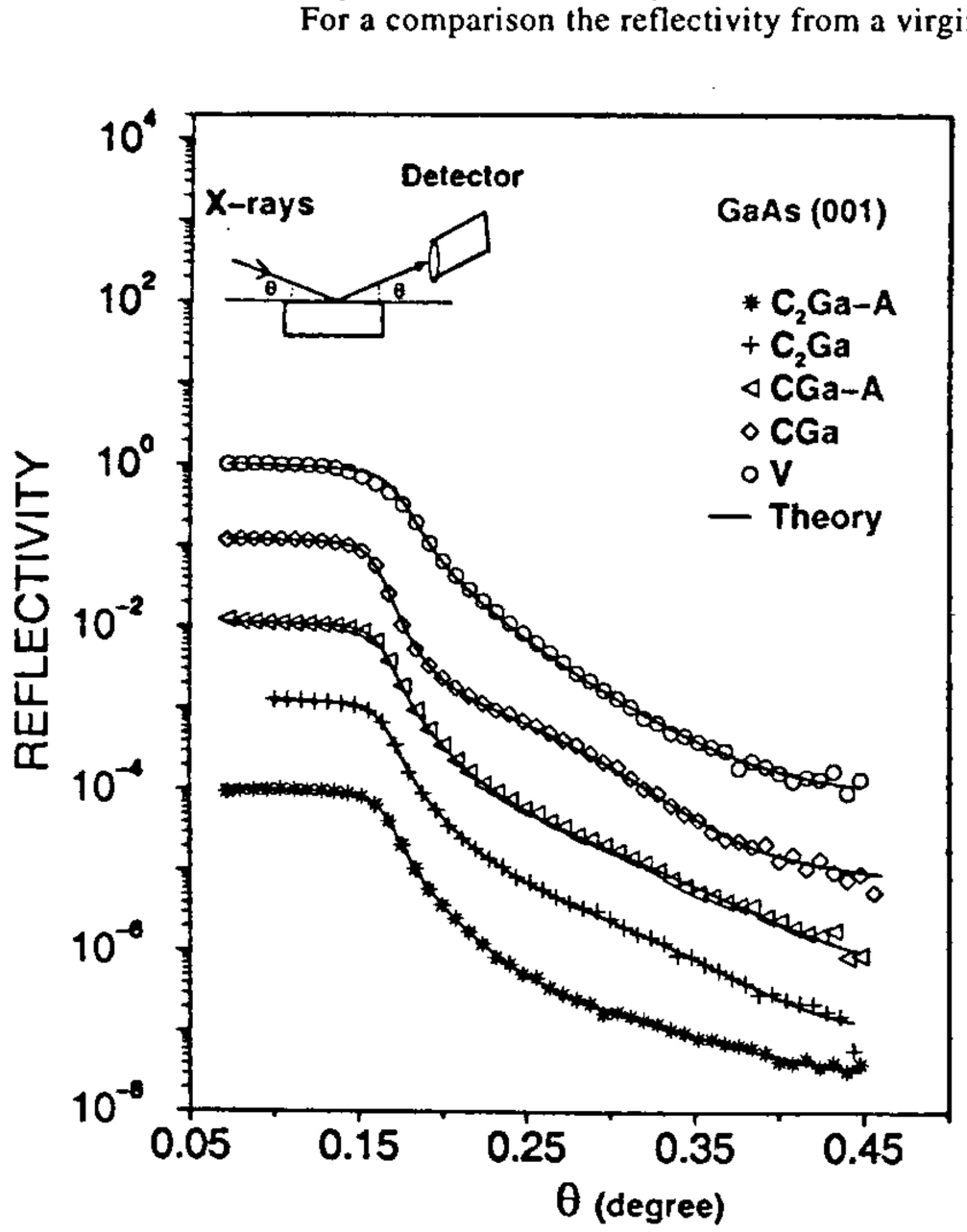

Figure 2. X-ray (MoK$_{\alpha 1}$) reflectivity for virgin GaAs(001) (V), C^+ and Ga^{2+} co-implanted GaAs(001) [as-implanted (CGa), annealed (CGa-A)], and C^+_2 and Ga^{2+} co-implanted GaAs(001) [as-implanted (C_2Ga), annealed (C_2Ga-A)] samples. The ordinates of the successive curves have been shifted by a decade for clarity. For CGa the oscillation on reflectivity corresponds to a 9.1 ± 0.1 nm top GaAs layer of ~ 9% reduced electron density. (From Ghose *et al.*[3]).

pseudomorphically, i.e. strained but without dislocations. For a layer thickness $t > t_c$ dislocations appear in the layer and the strain may be partially relieved. Beyond a certain thickness $t >> t_c$ the layer may be completely relaxed having no strain but a large dislocation density. It is important to determine the strain and dislocation density as a function of layer thickness to verify theories of epilayer growth and predictions of t_c. With HRXRD we determined the strain in a buried $CoSi_2$ epilayer in a sandwich system Si(111)/$CoSi_2$(111)/Si(111)[9]. Using other complementary techniques like ion scattering we studied other aspects of this buried epilayer system including determination of dislocation density[9]. Besides fundamental interests, this system, having Schottky barriers at both Si/$CoSi_2$ and $CoSi_2$/Si interfaces is a potential candidate for metal-base and permeable-base transistors.

Interface atomic structures

The atomic arrangements at an interface determine the interface properties. Experimentally determined interface atomic structures[10] have been used for the calculation[11] of interface electronic properties showing their dependence on interface atomic geometry. This shows the importance of the determination of interface atomic geometry. We have used the XSW technique to determine the structure of the $CoSi_2$(111)/Si(111) interfaces

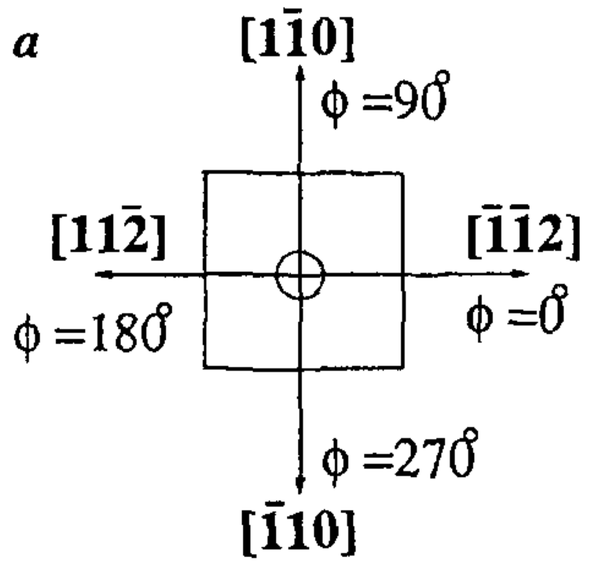

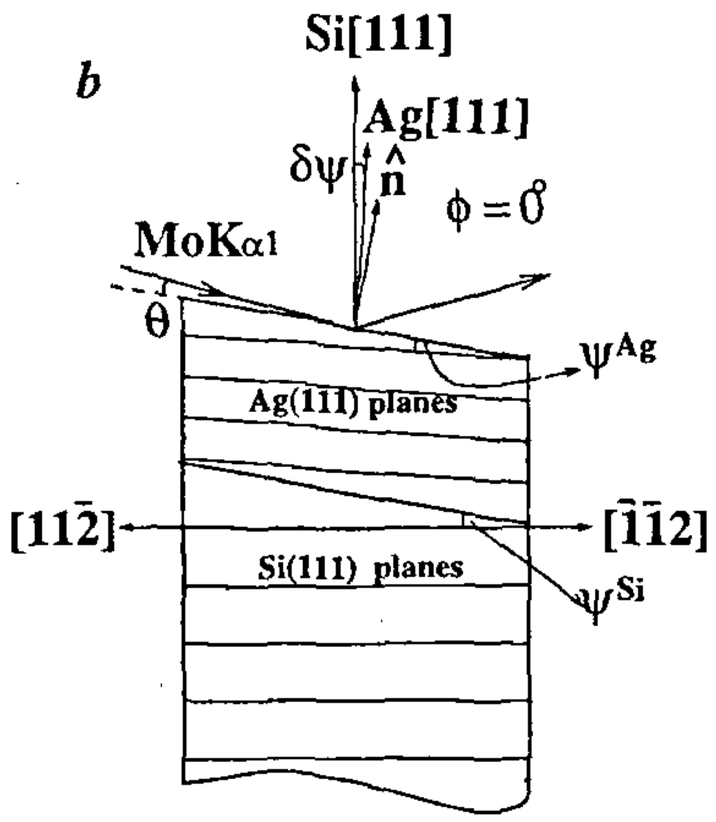

Figure 3. *a*, Top view of the sample showing azimuthal orientations; *b*, schematic diagram showing surface normal ($\hat{n}$), Ag(111) and Si(111) diffraction planes, asymmetry angles (ψ^{Si}) and ψ^{As}) and tilt ($\delta\psi$) between Si[111] and Ag[111] directions. ψ^{Si} (= 4°) is the miscut angle. (From Sundaravel *et al.*[8]).

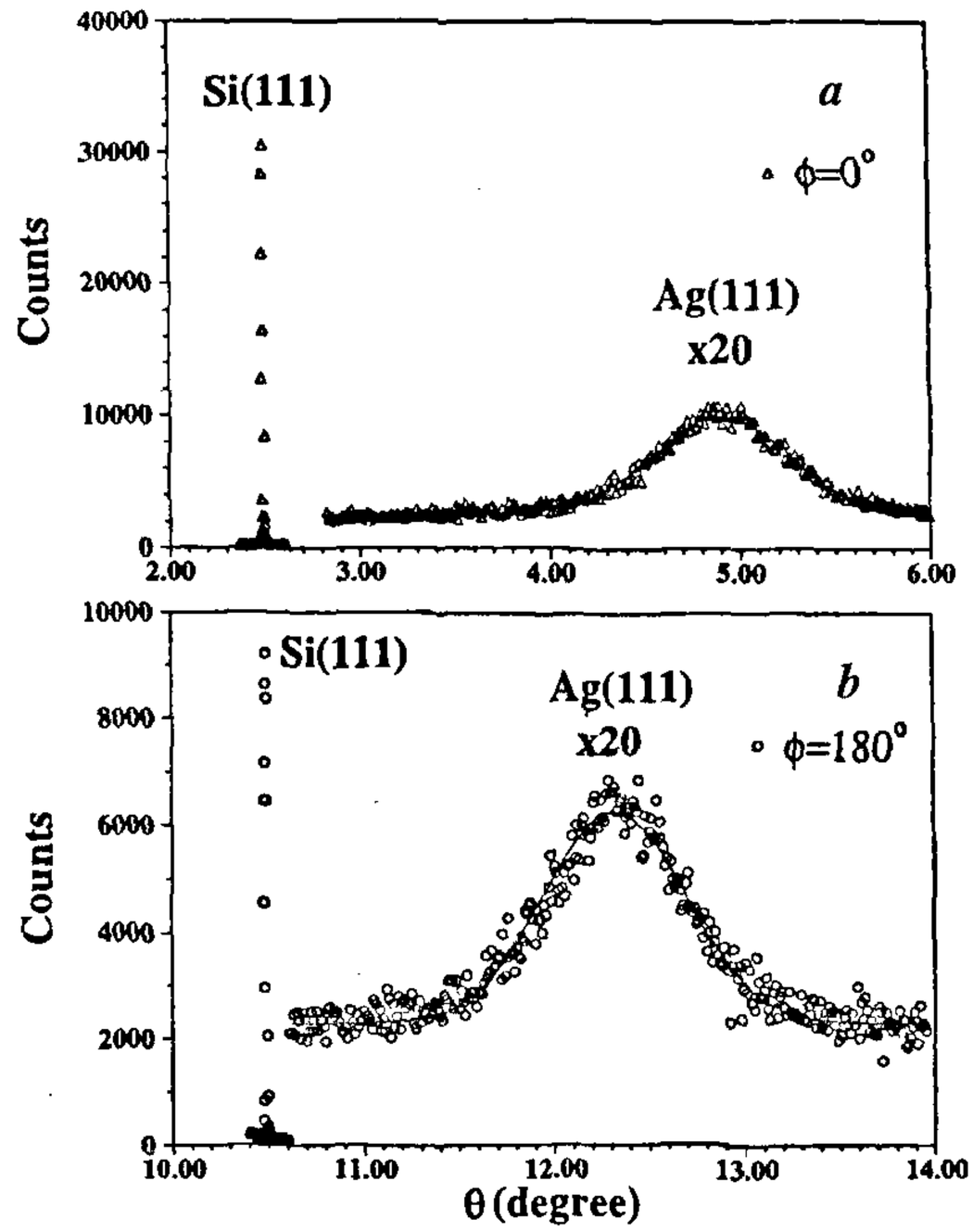

Figure 4. HRXRD results with $MoK_{\alpha 1}$ X-ray beam incident (*a*) towards [112] and (*b*) towards [$\bar{1}\bar{1}$2] directions. Note at what angles (θ) diffractions occur. [The Bragg angle (θ_B) for Si(111) reflection is 6.492°]. (From Sundaravel *et al.*[8]).

in the buried $Si/CoSi_2/Si(111)$ system[12]. The $Si/CoSi_2/Si$ system with sharp interfaces was prepared by ion implantation of Co into Si(111) crystals, that is, by ion beam synthesis[12]. In the usual ion implantation process the modified layer has a blurred interface. In such a case incorporation of implanted Au atoms into the $LiNbO_3$ lattice and the initiation of clustering have been studied by the XSW technique in conjunction with other techniques[13]. Formation of metallic clusters in dielectrics by metal ion implantation is an important method for the fabrication of nonlinear optical elements.

Chemisorption and desorption on surfaces

Surface atoms on a clean single crystal surface, because of the missing atoms on one side, experience different interactions compared to those deep inside the crystal. This often leads to new equilibrium surface atomic structures. That is to say, the surface is reconstructed. Often the effect of the missing atoms can be partly restored by chemisorption of a different kind of atom on the surface. This can remove the reconstruction. The behaviour of and the interactions on a surface can be understood through the studies of chemisorption and desorption processes and the related electronic properties. For example, a clean Si(111) surface is (7 × 7) reconstructed. Chemisorption of halogen atoms removes this reconstruction and brings it back to the (1 × 1) unreconstructed structure. Electronic structures of such chemisorbed systems[14] can be compared with those of the bare Si(111) (7 × 7) surface for a better understanding of surface interactions.

We studied bromine chemisorption and its desorption behaviour on silicon (111) and Si(100) surfaces by X-ray photoelectron spectroscopy (XPS). We identified a relationship between the desorption rate and the chemical shift of Br 3p levels[15]. The larger desorption rate on a Si(100) surface was attributed to the presence of two dangling bonds per surface Si atom, which are difficult to saturate by Br chemisorption due to a steric hindrance. On a Si(111) surface there is one dangling bond per surface Si atom and apparently no such problem arises[16]. A Br 3p photoelectron spectrum and the Br desorption behaviour are shown in Figure 5.

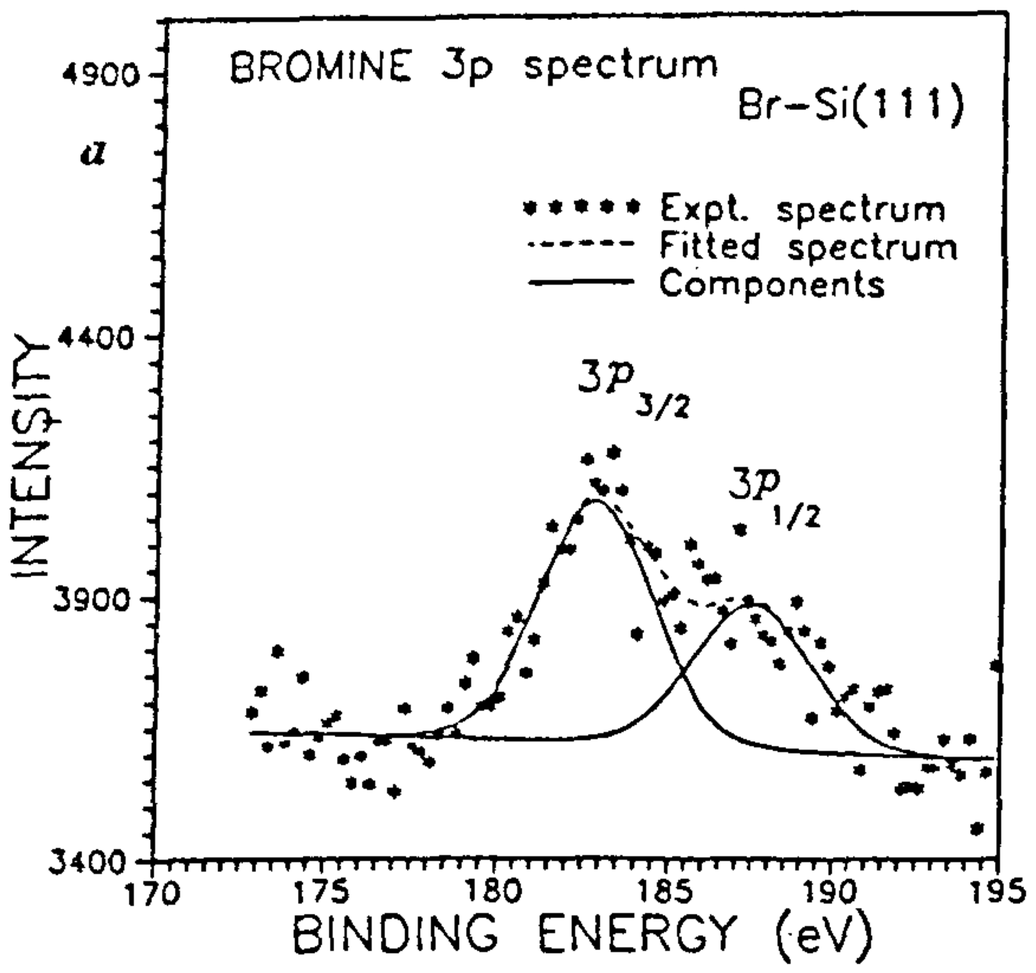

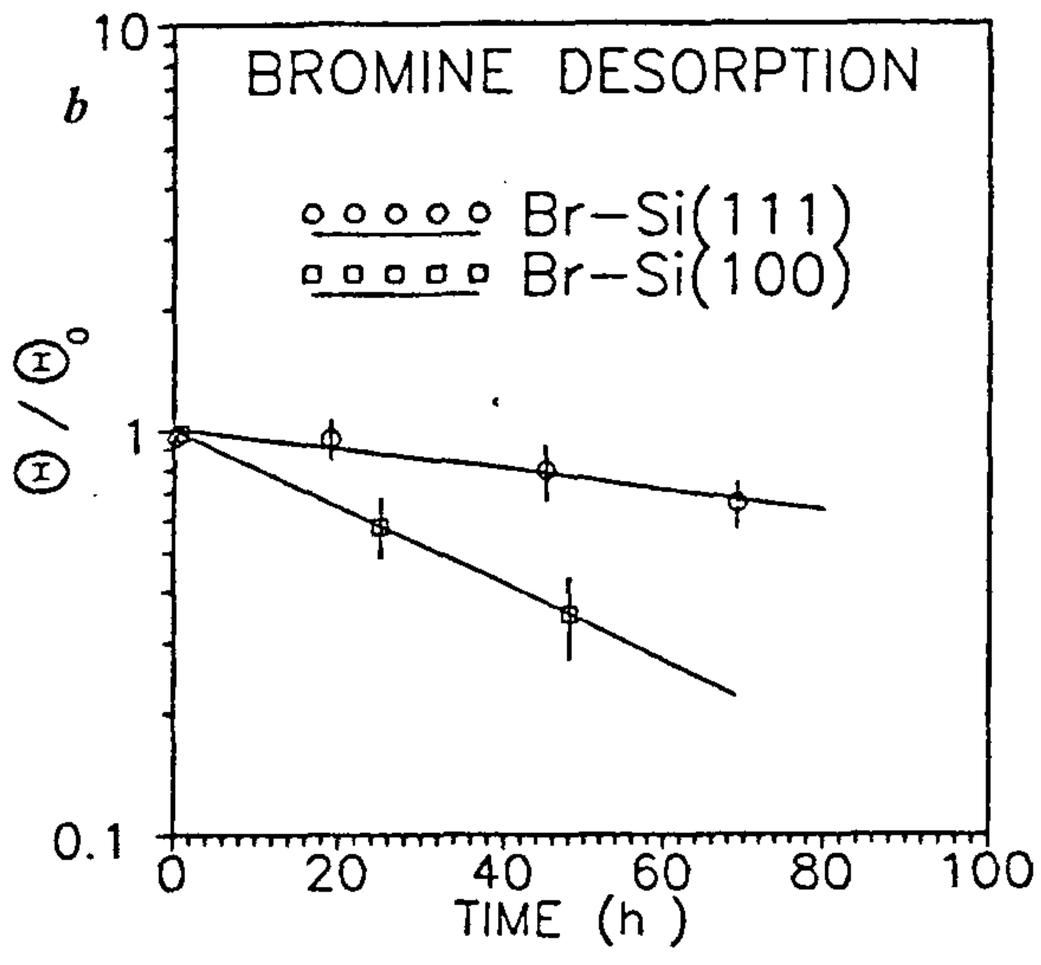

Figure 5. *a*, Br 3p photoelectron spectrum from a Br-adsorbed Si(111) surface; *b*, normalized Br coverage (θ/θ_0): the decreasing value with time indicates desorption [$\theta = \theta_0 \exp(-k_D t)$]. The desorption rate constants for Si(111) and Si(100) surfaces are 0.006 and 0.022 per hour, respectively. Initial Br coverage θ_0 ($\sim 5 \times 10^{14}$ atoms/cm^2) in both cases was less than one complete atomic layer. (From Sekar *et al.*[15]).

Conclusion

Here we have presented a brief account of our research activities in the area of surface and interface science limiting the discussions on X-ray characterizations. We are in the process of developing a molecular beam epitaxy (MBE) facility for growing high quality epitaxial layers under ultra-high vacuum conditions. The potentials of our X-ray characterization techniques, especially of XSW[17], could not be effectively utilized for the lack of an appropriate sample preparation facility. With a facility for MBE growth, this situation is expected to change in the near future.

1. Satyam, P. V. and Dev, B. N., *Indian J. Phys. A*, 1995, **69**, 415–425.
2. Satyam, P. V., Bahr, D., Ghose, S. K., Kuri, G., Sundaravel, B., Rout, B. and Dev, B. N., *Curr. Sci.*, 1995, **69**, 526–529.
3. Ghose, S. K., Kuri, G., Das, Amal, K., Rout, B., Mohapatra, D. P. and Dev, B. N., *Nucl. Instrum. Methods B*, 1999, **156**, 125–129.
4. Biersack, J. P. and Haggmark, L., *Nucl. Instrum. Methods*, 1980, **174**, 257, [TRIM (TRansport of Ions through Matter) code].
5. Sekar, K., Kuri, G., Satyam, P. V., Sundaravel, B., Mohapatra, D. P. and Dev, B. N., *Phys. Rev. B*, 1995, **51**, 14330.
6. Tersoff, J. and Tromp, R. M., *Phys. Rev. Lett.*, 1993, **70**, 2782–2785.
7. Brongersma, S. H., Castell, M. R., Perovic, D. D. and Zinke-Allmang, M., *Phys. Rev. Lett.*, 1998, **80**, 3795–3798.
8. Sundaravel, B., Das, Amal, K., Ghose, S. K., Sekar, K. and Dev, B. N., *Appl. Surf. Sci.*, 1999, **137**, 11–19.
9. Dev, B. N., *Nucl. Instrum. Methods B*, 1999, **156**, 258–264, and references therein.
10. Vlieg, E., Fischer, A. E. M. J., Van der Veen, J. F., Dev, B. N. and Materlik, G., *Surf. Sci.*, 1986, **178**, 36–46.
11. Das, G. P., Brochl, P., Anderson, O. K., Christensen, N. E. and Gunnarsson, O., *Phys. Rev. Lett.*, 1989, **63**, 1168–1171.
12. Satyam, P. V. and Dev, B. N., *Indian J. Phys. A*, 1994, **68**, 23–32.
13. Dev, B. N., Kuri, G., Satyam, P. V., Sundaravel, B., Gog, Th. and Materlik, G., *Appl. Surf. Sci.*, 1998, **125**, 163–172.
14. Dev, B. N., Mishra, K. C., Gibson, W. M. and Das, T. P., *Phys. Rev. B*, 1984, **29**, 1101–1104.
15. Sekar, K., Kuri, G., Mahapatra, D. P., Dev, B. N., Ramana, J. V., Kumar, S. and Raju, V. S., *Surf. Sci.*, 1994, **302**, 25–36.
16. Sekar, K., Satyam, P. V., Kuri, G., Mahapatra, D. P. and Dev, B. N., *Nucl. Instrum. Methods B*, 1992, **71**, 308–313.
17. See for example, Dev, B. N., Materlik, G., Grey, F., Johnson, R. L. and Clausnitzer, M., *Phys. Rev. Lett.*, 1986, **57**, 3058–3061.